Stability analysis of collective neutrino oscillations in the supernova accretion phase with realistic energy and angle distributions

Ninetta Saviano, Sovan Chakraborty, Tobias Fischer, and Alessandro Mirizzi

Phys. Rev. D **85**, 113002 — Published 4 June 2012

DOI: 10.1103/PhysRevD.85.113002

Stability analysis of collective neutrino oscillations in the supernova accretion phase with realistic energy and angle distributions

Ninetta Saviano,[1] Sovan Chakraborty,[1] Tobias Fischer,[2,3] and Alessandro Mirizzi[1]

[1] *II Institut für Theoretische Physik, Universität Hamburg, Luruper Chaussee 149, 22761 Hamburg, Germany*

[2] *GSI, Helmholtzzentrum für Schwerionenforschung GmbH, Planckstraße 1 64291 Darmstadt, Germany*

[3] *Technische Universität Darmstadt, Schlossgartenstraße 9, 64289 Darmstadt, Germany*

We revisit our previous results on the matter suppression of self-induced neutrino flavor conversions during a supernova (SN) accretion phase, performing a linearized stability analysis of the neutrino equations of motion, in the presence of realistic SN density profiles. In our previous numerical study, we used a simplified model based on an isotropic neutrino emission with a single typical energy. Here, we take into account realistic neutrino energy and angle distributions. We find that multi-energy effects have a sub-leading impact in the flavor stability of the SN neutrino fluxes with respect to our previous single-energy results. Conversely, realistic forward-peaked neutrino angular distributions would enhance the matter suppression of the self-induced oscillations with respect to an isotropic neutrino emission. As a result, in our models for iron-core SNe, collective flavor conversions have a negligible impact on the characterization of the observable neutrino signal during the accretion phase. Instead, for a low-mass O-Ne-Mg core SN model, with lower matter density profile and less forward-peaked angular distributions, collective conversions are possible also at early times.

PACS numbers: 14.60.Pq, 97.60.Bw

I. INTRODUCTION

Supernova (SN) neutrinos are important astrophysical messengers to probe the flavor mixing in unique conditions [1, 2]. In particular, renewed attention is being paid to collective features of flavor transformations [3–15] induced by ν-ν self-interactions [16–18] in the deepest stellar regions, near the neutrino-sphere. The observed collective phenomena of synchronized [19] and pendular [20] oscillations, and the splits [21–23] in the observable SN neutrino spectra are subjects of intense investigations (see [24] for a recent review).

The implicit assumption in the characterization of the self-induced oscillations is related to the flavor evolution in the deepest SN regions, being driven by the only large neutrino densities n_ν. However, during the SN accretion phase (at post-bounce times $t_{\rm pb} \lesssim 0.5$ s) also the net electron density n_e is expected to be large. As pointed out in [25], when n_e is not negligible with respect to n_ν, the large phase dispersion induced by the matter for ν's traveling in different directions, would partially or totally suppress the collective oscillations through peculiar "multi-angle effects". At this regard, in two previous papers [26, 27] we performed a numerical study of the matter suppression during the accretion phase, characterizing the matter and the neutrino density profiles with the results from recent long-term SN hydrodynamical simulations [28], based on three flavor Boltzmann neutrino transport in spherical symmetry. Multi-angle numerical simulations of the non-linear neutrino equations of motion in the presence of large neutrino and matter densities are computationally very demanding. Indeed, these equations are "stiff" and their solutions generally involve a fast-changing combination of multi-frequency oscillations. In order to reduce this numerical complexity, we assumed a simplified neutrino emission model. Namely, we considered all the neutrinos to be emitted "half-isotropically" (i.e. with all outward-moving angular modes equally occupied and all the backward-moving modes empty) from a common neutrino-sphere with a single representative energy. In this framework, we found that the presence of a dominant matter term inhibits the development of collective flavor conversions. The matter suppression ranges from complete (when $n_e \gg n_\nu$) to partial (when $n_e \gtrsim n_\nu$) suggesting, in principle, time-dependent features. In particular, for the iron-core SN models we analyzed, we found complete matter suppression of the collective oscillations for post-bounce times $t_{\rm pb} \lesssim 0.2$ s and $t_{\rm pb} \gtrsim 0.4$ s and partial flavor conversions (with electron antineutrino survival probability $P_{ee} \simeq 0.5$) in the intermediate time range.

Our works have stimulated further independent investigations of these effects [29–31]. In particular, in [30] it has been proposed to study the matter suppression of the self-induced oscillations applying the linearized stability analysis of the neutrino equations of motion, recently worked out in [32]. This method is particularly useful to circumvent the challenges of full numerical multi-angle simulations for the flavor evolution. These are not necessary if one is interested only in the issue of the flavor stability of the dense neutrino gas. Indeed, the stability analysis would allow one to determine the possible onset of the flavor conversions, seeking for an exponentially growing solution of the eigenvalue problem, associated with the linearized equations of motion for the neutrino ensemble. With this approach, taking as benchmark for the SN density profiles and for the neutrino emission a 15.0 $M_\odot$ iron-core SN model from the Garching group, the stability analysis has shown a complete suppression of the collective oscillations for all the duration of the ac-

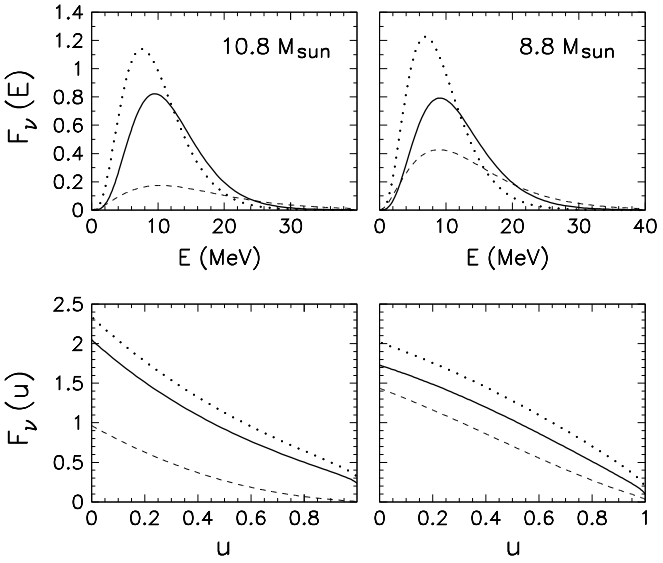

FIG. 1: Supernova neutrino flux spectra (in arbitrary units) for 10.8 $M_\odot$ progenitor at $t_{\rm pb} = 0.225$ s (left panels) and for 8.8 $M_\odot$ progenitor at $t_{\rm pb} = 0.250$ s (right panels). The energy (upper panels) and the angular (lower panels) spectra are shown for ν_e (dotted curves), $\overline{\nu}_e$ (continuous curves) and ν_x (dashed curves) (see the text for details).

cretion phase [30]. Subsequently, the same technique has been applied to our numerical results [31], finding perfect agreement with our sequence of complete and partial matter suppression.

Motivated by these interesting papers, we find useful to improve our previous results applying the stability analysis to our models, including also realistic energy and angle neutrino distributions. The plan of our work is as follows. In Sec. 2 we introduce the SN models used to characterize the SN densities and, the neutrino energy and angle fluxes. In Sec. 3 we introduce the setup for the flavor-stability analysis, describing the non-linear equations for the neutrino flavor evolution in SNe, and the consistency equations coming from their linearization. In Sec. 4 we present our results for the stability analysis of the matter suppression during the accretion phase for two different SN progenitor masses. Finally, in Sec. 5 we comment on our results and we conclude.

II. SUPERNOVA MODELS

We considered the core-collapse supernova simulations of massive progenitor stars with 8.8 and 10.8 $M_\odot$ progenitor from Ref. [28], taken as benchmark for our numerical study in [27]. The first SN belongs to the class of O-Ne-Mg-core progenitors [33, 34] and represents the threshold between thermonuclear explosions and core-collapse supernovae [28, 35]. The second is an iron-core progenitor [36]. All models were evolved consistently through core collapse, bounce and the early post-bounce phase up to several seconds after the onset of explosion [28]. We remind that in order to trigger the explosion for the 10.8 $M_\odot$ progenitor model, the heating rates have been artificially enhanced in the gain region where neutrinos deposit energy in order to revive the stalled bounce shock.

In our previous study, we schematically took a mono-energetic ν ensemble, with a representative energy $E = 15$ MeV. Neutrinos of different species were assumed to be emitted half-isotropically by a common spherical "neutrino-sphere," in analogy with a blackbody emission. However, realistic supernova simulations show that ν angular distributions at the decoupling are far from being half-isotropic and are flavor-dependent (see, e.g., [30, 37]). In order to fix a common neutrino-sphere radius $r = R$ for the flavor evolution, consistently with our choice in [27] we take the radius at which the ν_e's angular distribution has no longer significant backward flux, i.e. a few % of the total one. This typically is in the range $R \sim 50 - 100$ km (see Fig. 4 in [27]). It is convenient to parameterize every angular mode in terms of its emission angle θ_R relative to the radial direction of the neutrino-sphere. For a half-isotropic distribution the occupation numbers are distributed as $dn/d\cos\theta_R =$ const, or equivalently the radial fluxes are distributed as $dF/d\cos\theta_R \propto \cos\theta_R$ [38]. A further simplification is obtained if one labels the different angular modes in terms of the variable $u = \sin^2\theta_R$, as in [32, 38]. Note that for a half-isotropic emission at the neutrino-sphere the ν angular distribution of the radial fluxes is a box spectrum in $0 \leq u \leq 1$, since $d\cos\theta_R/du \propto (\cos\theta_R)^{-1}$ cancels the $\cos\theta_R$ dependence previously mentioned.

From SN simulations of [28] we extract the angle and energy distributions $F_{\nu_\alpha}(E,u)$ of the different neutrino species. In Fig. 1 we show the (angle-integrated) flux energy spectra $F_{\nu_\alpha}(E)$ (upper panels) and the (energy-integrated) flux angular spectra $F_{\nu_\alpha}(u)$ (lower panels) for ν_e, $\overline{\nu}_e$, ν_x, where this latter indicates the non-electron flavors. Here, we are showing these fluxes for the 10.8 $M_\odot$ SN progenitor at $t_{\rm pb} = 225$ ms (left panels), and for the 8.8 $M_\odot$ SN progenitor at $t_{\rm pb} = 250$ ms (right panels). The angular variable $0 \leq u \leq 1$ is based on $R = 69$ km for the 10.8 $M_\odot$ model, and on $R = 47$ km for the 8.8 $M_\odot$ model. The energy and angular distributions are normalized to the total neutrino number fluxes of the different species (in arbitrary units in the Figure).

Concerning the neutrino energy distributions for the different flavors, the angle-integrated energy spectra are well-represented by the renowned form [39, 40]

$$F_{\nu_\alpha}(E) = \frac{L_\nu}{\langle E_\nu\rangle^2}\frac{(1+\beta)^{1+\beta}}{\Gamma(1+\beta)}\left(\frac{E}{\langle E_\nu\rangle}\right)^\beta \exp\left[-(1+\beta)\frac{E}{\langle E_\nu\rangle}\right], \quad (1)$$

where for a given flavor L_ν is the neutrino luminosity, $\langle E_\nu\rangle$ is the average energy and β is the energy-shape

parameter, defined as [39, 40]

$$\beta = \frac{2\langle E_\nu\rangle^2 - \langle E_\nu^2\rangle}{\langle E_\nu^2\rangle - \langle E_\nu\rangle^2}\,, \tag{2}$$

i.e. it is a dimensionless parameter containing information on the second moment of the distribution, $\langle E_\nu^2\rangle$. In general, L_ν, $\langle E_\nu\rangle$ and $\langle E_\nu^2\rangle$ are all functions of time, and are extracted directly from the simulations at hand (see Fig. 2 in [28]). In the case of 10.8 $M_\odot$ we find a typical total number flux hierarchy expected during the accretion phase, numerically $F_{\nu_e} : F_{\overline{\nu}_e} : F_{\nu_x} = 1.20 : 1.00 : 0.34$. The first part of the hierarchy is caused by the deleptonization of the collapsed core whereas the second is caused by the absence of charged current interactions for neutrino species other than ν_e and $\overline{\nu}_e$. Passing now to the case of the low-mass 8.8 $M_\odot$ SN progenitor, we realize that the spectrum of the non-electron flavors is less suppressed with respect to the electron (anti)neutrino spectra, namely $F_{\nu_e} : F_{\overline{\nu}_e} : F_{\nu_x} = 1.23 : 1.00 : 0.72$. This different behavior is due to the fact that in low-mass core SNe, the duration of the accretion phase is very short (i.e. $t_{\rm pb} \lesssim 0.03$ s in Fig. 2 of Ref. [28]). At later times, the neutrino luminosities can be approximated by diffusion and the spectra are determined from thermalization processes (e.g., inelastic scattering on electrons/positrons and elastic scattering on nucleons). Since these neutral-current processes do not distinguish the different flavors, this leads to reduced spectral differences between electron and non-electron species (see, e.g., [41]).

Considering now to the angular flux spectra, we realize that in the case of the 10.8 $M_\odot$ model, these are significantly forward enhanced (i.e. peaked at small u), with respect to the half-isotropic emission model. Remarkably, the angular distributions of the three ν species at the conventional neutrino-sphere are rather different: since the ν_x's decouple at smaller radii with respect to ν_e's and $\overline{\nu}_e$'s, their distributions are more suppressed in the direction tangential to the neutrino-sphere (i.e. at $u \sim 1$). In the case of 8.8 $M_\odot$ the angular spectra for the electron species are less forward-enhanced than in the previous case, and with less pronounced differences with the non-electron species. As for the energy spectra, this behavior is due to the dominant role of the neutral-current processes in the spectra formation. We also note that for the models we considered the angular distributions do not cross at any u. [1]

[1] As recently discussed in [42], possible crossings in the angular distributions of different flavors could lead to an enhancement of the flavor instability.

III. SETUP OF THE STABILITY ANALYSIS

A. Equations of motion

We work in a two-flavor oscillation scenario, associated to the atmospheric mass-square difference $\Delta m^2_{\rm atm} = 2\times10^{-3}$ eV^2 and and with the small (matter suppressed) in-medium mixing $\Theta_{\rm eff} = 10^{-3}$ [43]. We will always assume inverted mass hierarchy ($\Delta m^2_{\rm atm} < 0$) where ν's can exhibit flavor instabilities for the flux ordering present during the accretion phase [6]. For this flux hierarchy, three-flavor effects, associated with the solar mass splitting are negligible [7]. Following [32], we write the equations of motion for the flux matrices $\Phi_{E,u}$ as function of the radial coordinate. The diagonal $\Phi_{E,u}$ elements are the ordinary number fluxes $F_{\nu_\alpha}(E,u)$ integrated over a sphere of radius r. We normalize the flux matrices to the total $\overline{\nu}_e$ number flux $n_{\overline{\nu}_e}$ at the neutrino-sphere. Conventionally, we use negative E and negative number fluxes for anti-neutrinos. The off-diagonal elements, which are initially zero, carry a phase information due to flavor mixing. Then, the equations of motion read [32, 44]

$$\mathrm{i}\partial_r \Phi_{E,u} = [H_{E,u}, \Phi_{E,u}] \tag{3}$$

with the Hamiltonian [18, 32, 44, 45]

$$H_{E,u} = \frac{1}{v_u}\left(\frac{M^2}{2E} + \sqrt{2}G_F N_l\right) + \frac{\sqrt{2}G_F}{4\pi r^2}\int_{-\infty}^{+\infty} dE' \int_0^1 du' \left(\frac{1 - v_u v_{u'}}{v_u v_{u'}}\right)\Phi_{E',u'}\ . \tag{4}$$

The matrix M^2 of neutrino mass-squares causes vacuum flavor oscillations. The matrix $N_l = \mathrm{diag}(n_e, 0, 0)$ in flavor basis, contains the net electron density and is responsible for the Mikheyev-Smirnov-Wolfenstein (MSW) matter effect [46] with the ordinary background. Finally, the term at second line represents the ν-ν refractive term. In particular, the factor proportional to the neutrino velocity $v_u = (1 - uR^2/r^2)^{1/2}$ [38] in the ν-ν interaction term implies "multi-angle" effects for neutrinos moving on different trajectories [5, 18, 44, 45]. In order to properly simulate numerically this effect one needs to follow a large number [$\mathcal{O}(10^3)$] of interacting neutrino modes.

B. Stability conditions

In order to perform the stability analysis we closely follow the prescriptions presented in [32] and summarized in the following. At first we switch to the frequency variable $\omega = \Delta m^2_{\rm atm}/2E$ so that $E(\omega) = |\Delta m^2_{\rm atm}/2\omega|$ and we introduce the neutrino flux difference distributions $g_{\omega,u} \equiv g(\omega,u)$ defined as

$$g_{\omega,u} = \frac{|\Delta m^2_{\rm atm}|}{2\omega^2} \times \Big\{\Theta(\omega)\left[F_{\nu_e}(E(\omega),u) - F_{\nu_x}(E(\omega),u)\right] + \Theta(-\omega)\left[F_{\nu_x}(E(\omega),u) - F_{\overline{\nu}_e}(E(\omega),u)\right]\Big\} \tag{5}$$

normalized to the total $\overline{\nu}_e$ flux at the neutrino-sphere. Then, we write the flux matrices in the form [32]

$$\Phi_{\omega,u} = \frac{\mathrm{Tr}\Phi_{\omega,u}}{2} + \frac{g_{\omega,u}}{2} \begin{pmatrix} s_{\omega,u} & S_{\omega,u} \\ S^*_{\omega,u} & -s_{\omega,u} \end{pmatrix} \ , \qquad (6)$$

where $\mathrm{Tr}\Phi_{\omega,u}$ is conserved and then irrelevant for the flavor conversions, and the initial conditions for the "swapping matrix" in the second term on the right-hand side are $s_{\omega,u} = 1$ and $S_{\omega,u} = 0$. Self-induced flavor transitions start when the off-diagonal term $S_{\omega,u}$ grows exponentially.

In the small-amplitude limit $|S_{\omega,u}| \ll 1$, and at far distances from the neutrino-sphere $r \gg R$, the linearized evolution equations for $S_{\omega,u}$ in inverted mass hierarchy ($\Delta m^2_{\rm atm} < 0$) assume the form [32]

$$\begin{aligned} \mathrm{i}\partial_r S_{\omega,u} &= [\omega + u(\lambda + \epsilon\mu)] S_{\omega,u} \\ &- \mu \int du' d\omega' (u + u') g_{\omega',u'} S_{\omega',u'} \ , \end{aligned} \qquad (7)$$

where

$$\epsilon = \int du \ d\omega \ g_{\omega,u} \ , \qquad (8)$$

quantifies the "asymmetry" of the neutrino spectrum, normalized to the total $\overline{\nu}_e$ number flux. The ν-ν interaction strength is given by

$$\begin{aligned} \mu &= \frac{\sqrt{2} G_F n_{\bar{\nu}_e}(R)}{4\pi r^2} \frac{R^2}{2r^2} \\ &= \frac{3.5 \times 10^9}{r^4} \left(\frac{L_{\overline{\nu}_e}}{10^{52} \ \mathrm{erg/s}} \right) \left(\frac{15 \ \mathrm{MeV}}{\langle E_{\overline{\nu}_e} \rangle} \right) \left(\frac{R}{10 \ \mathrm{km}} \right)^2 , \end{aligned}$$

while ordinary matter background term is given by

$$\begin{aligned} \lambda &= \sqrt{2} G_F n_e \frac{R^2}{2r^2} \\ &= \frac{0.95 \times 10^8}{r^2} \left(\frac{Y_e}{0.5} \right) \left(\frac{\rho}{10^{10} \mathrm{g/cm^3}} \right) \left(\frac{R}{10 \ \mathrm{km}} \right)^2 , \end{aligned}$$

where Y_e is the net electron fraction, and ρ is the matter density. The radial distance r is expressed in km, while the numerical values of μ and λ in the two previous equations are quoted in km^{-1}, as appropriate for the SN case.

One can write the solution of the linear differential equation [Eq. (7)] in the form $S_{\omega,u} = Q_{\omega,u} e^{-i\Omega r}$ with complex frequency $\Omega = \gamma + i\kappa$ and eigenvector $Q_{\omega,u}$. A solution with $\kappa > 0$ would indicate an exponential increasing $S_{\omega,u}$, i.e. an instability. The solution of Eq. (7) can then be recast in the form of an eigenvalue equation for $Q_{\omega,u}$. Splitting this equation into its real and imaginary parts one arrives at two real equations that have to be satisfied [32]

$$\begin{aligned} (J_1 - \mu^{-1})^2 &= K_1^2 + J_0 J_2 - K_0 K_2 \ , \\ (J_1 - \mu^{-1}) &= \frac{J_0 K_2 + K_0 J_2}{2K_1} \ , \end{aligned} \qquad (9)$$

where

$$\begin{aligned} J_n &= \int d\omega du \ g_{\omega,u} u^n \frac{\omega + u(\lambda + \epsilon\mu) - \gamma}{[\omega + u(\lambda + \epsilon\mu) - \gamma]^2 + \kappa^2} \ , \\ K_n &= \int d\omega du \ g_{\omega,u} u^n \frac{\kappa}{[\omega + u(\lambda + \epsilon\mu) - \gamma]^2 + \kappa^2} . \end{aligned} \qquad (10)$$

A flavor instability is present whenever Eqs. (9) admit a solution (γ, κ).

IV. APPLICATION TO OUR SUPERNOVA MODELS

In this Section we will present our results for the stability analysis of the self-induced flavor conversions for two representative SN simulations based on different progenitor masses.

A. 10.8 $\mathrm{M}_\odot$ progenitor mass

We start our investigation with the case of the 10.8 $\mathrm{M}_\odot$ iron-core supernova. We briefly remind the reader our previous results presented in Ref. [27]. For this SN model, the net electron density n_e and the neutrino densities n_ν for different post-bounce times were shown in Fig. 5 of our previous paper [27]. The numerical results of the multi-angle flavor evolution for our schematic model with neutrinos of different species all emitted half-isotropically with a single energy, were shown in Fig. 7. In particular, it was represented the survival probability of electron antineutrinos P_{ee}, at different post-bounce times in the presence of matter effects and for $n_e = 0$. The matter effects produced a complete suppression of the flavor conversions for $t_{\rm pb} \lesssim 0.2$ s and $t_{\rm pb} \gtrsim 0.4$ s (where $n_e/n_{\bar{\nu}_e} \gg 1$, see Fig. 8 in [27]) and partial flavor conversions (with electron-survival probability $P_{ee} \simeq 0.5$) at the intermediate times (where $n_e/n_{\bar{\nu}_e} \gtrsim 1$).

We now compare these numerical results with what we find using the stability analysis. For the same post-bounce times considered in our previous paper, we show in Fig. 2 the radial evolution of the eigenvalue κ determined from the solution of Eqs. (9). We consider the following cases: *(a)* $n_e = 0$ and a half-isotropic neutrino emission (dashed curves), *(b)* dense matter effects and a half-isotropic neutrino emission (continuous curves) and, *(c)* dense matter effects and non-trivial neutrino angular distributions (dotted curves). In all these cases we have always assumed quasi-thermal neutrino energy distributions, parametrized as in Eq. (1).

We start discussing our results for the case of $n_e = 0$. We realize that when the neutrino system enters into an unstable regime ($\kappa > 0$), the κ function rapidly grows from zero to a peak value greater than one. Comparing this result with the numerical solution presented in Fig. 7 of [27], we find perfect agreement between the onset of the self-induced flavor conversions determined numerically and the position of the peak in the κ function.

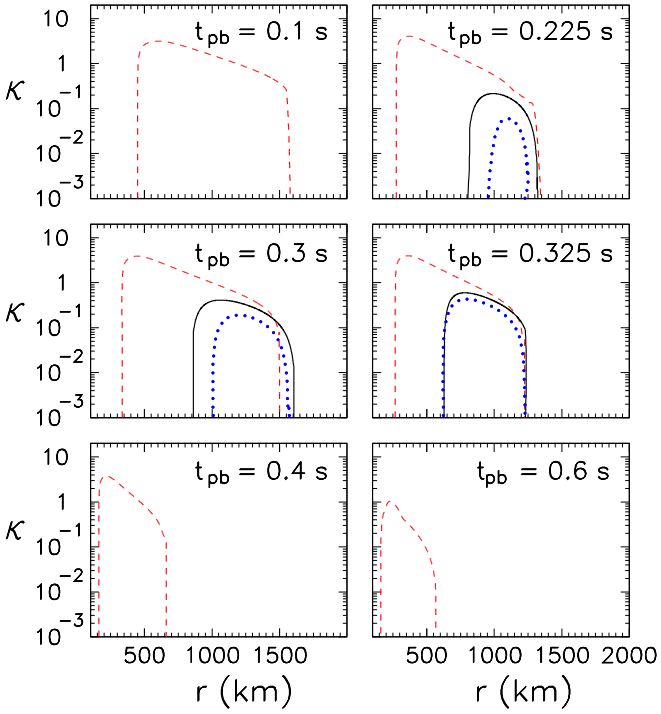

FIG. 2: 10.8 $M_\odot$ progenitor mass. Radial evolution of the κ function at different post-bounce times with $n_e = 0$ for a half-isotropic neutrino emission (dashed curves) and in presence of matter effects, with a half-isotropic neutrino emission (continuous curves) and with flavor-dependent angular distributions (dotted curves). Quasi-thermal ν energy spectra are assumed (see the text for details).

Remarkably, the multi-energy effects included in the stability analysis do not seem to produce major changes in the onset of the flavor conversions with respect to what observed in our previous mono-energetic investigation. Of course, once conversions are triggered, multi-energy effects would play a crucial role in determining the splitting features in the final neutrino spectra. For their characterization, multi-energy and multi-angle simulations of the flavor evolution are mandatory (see, e.g., [14]).

We now discuss the case with realistic matter density profiles and a half-isotropic neutrino emission. As expected, the flavor instability is strongly suppressed with respect to the previous case with $n_e = 0$. In particular, the κ function is non-zero only at intermediate post-bounce times, i.e. $t_{\rm pb} = 0.225, 0.3, 0.325$ s in Fig. 2, consistently with the occurrence of the flavor conversions in [27]. In these cases the rise of the κ function is shifted at larger radii (by $\sim 400 - 500$ km) with respect to the case with $n_e = 0$. In particular, the instability occurs when $n_e \sim n_{\bar{\nu}_e}$. Moreover, the peak value of κ in these cases reaches at most ~ 0.5, implying a slower growth of the instability with respect to the case with $n_e = 0$. In the intermediate time snapshots, where the flavor conversions are not completely suppressed, we find an agreement between the onset of Fig. 7 in [27] and the position of the peak in the κ function.

Finally, we consider the case in which also the flavor-dependent forward-peaked neutrino angular distributions are taken into account. We find that the κ function is further suppressed with respect to the half-isotropic case. This is consistent with the expectation that the ν-ν strength is weaker for forward-peaked distributions, making the system more stable under the effect of the matter. We also note that at $t_{\rm pb} = 0.325$ s when the accretion is at the end, the effect of the angular-distributions is less pronounced, since these become less forward-enhanced, as discussed in Sec. 2.

In order to validate these findings we also performed multi-angle and multi-energy simulations of the flavor evolution, for the cases with realistic matter densities and neutrino energy and angle distributions. We used $N_u = 1200$ angular modes and $N_E = 80$ energy modes. Our main goal is to determine if flavor conversions are present or not, without being interested in the exact final outcome of the numerical simulations. Therefore, we did not require the perfect numerical convergence of our results. In the cases in which we have not found a positive κ with the stability analysis, also the numerical evolution has shown no flavor conversion. Moreover at $t_{\rm pb} = 0.225$ s, where $\kappa < 0.1$, the numerical simulation gives a complete suppression of the flavor conversions. Conversely, for the two other post-bounce times ($t_{\rm pb} = 0.3, 0.325$ s) where κ reaches a peak between 0.2 and 0.4, we find partial flavor conversions. However, in runs with different numbers of angular and energy modes the final value of P_{ee} ranges between $\sim 0.8 - 0.9$, suggesting that these partial flavor conversions would be practically negligible in the characterization of the supernova neutrino signal during the accretion phase.

Finally, we mention that we applied the stability analysis also to the case of a 18.0 $M_\odot$ iron-core supernova, considered in [27]. However, since the results obtained are similar to the ones discussed in this Section, for the sake of the brevity, we do not show them here.

B. 8.8 $M_\odot$ progenitor mass

We now analyze the case of a SN with a low-mass 8.8 $M_\odot$ O-Ne-Mg core. We remind that in this case there is an absence of an extended accretion phase, since the explosion succeeds very shortly after the core-bounce. For this model, the net electron density n_e and the neutrino densities n_ν at different post-bounce times ($t_{\rm pb} \leq 0.25$ s) are shown in Fig. 11 of [27]. The numerical results of the multi-angle flavor evolution for our schematic model with neutrinos emitted half-isotropically with a single energy were shown in Fig. 13 of [27]. From this Figure one can realize that the matter suppression of self-induced flavor conversions is never complete, since the matter density is very low with respect to iron-core progenitor. In Fig. 3 we plot the corresponding radial evolution of the κ function, for the *(a)*, *(b)*, *(c)* cases introduced in the previous

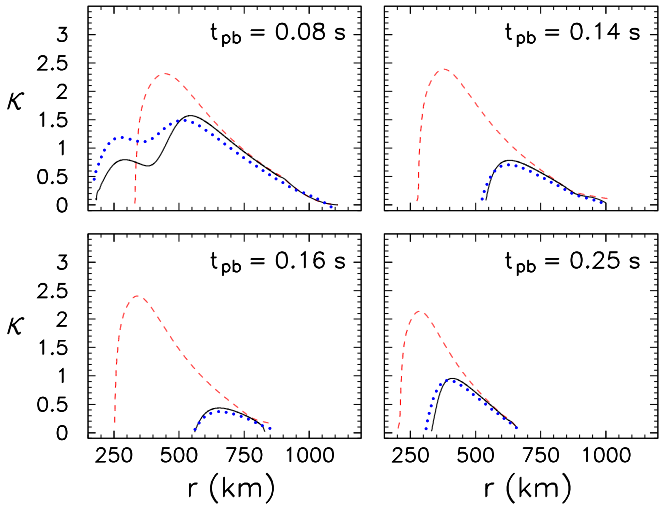

FIG. 3: 8.8 $M_\odot$ progenitor mass. Radial evolution of the κ function at different post-bounce times with $n_e = 0$ for a half-isotropic neutrino emission (dashed curves) and in presence of matter effects, with a half-isotropic neutrino emission (continuous curves) and with flavor-dependent angular distributions (dotted curves). Quasi-thermal ν energy spectra are assumed (see the text for details).

Section. In the case of a half-isotropic neutrino emission with $n_e = 0$ (dashed curves) we find once more a perfect agreement between the peak of the κ function and the onset of the flavor transitions found numerically.

We now discuss the matter effects. At first, we realize that the presence of non-trivial angular distributions (dotted curves) does not lead to a further suppression of the instability with respect to the case with a half-isotropic emission (continuous curves). This different behavior with respect to what we have seen in the case of 10.8 $M_\odot$ SN model, is consistent with what is shown in Fig. 1, i.e. the angular spectra of different flavors for the 8.8 $M_\odot$ SN are significantly less forward-peaked than in the case of the 10.8 $M_\odot$ SN. Therefore, their effect on the flavor stability is less pronounced. Looking in details at the different time snapshots in Fig. 3, we realize that at $t_{\rm pb} = 0.08$ s (when $n_{\bar\nu_e} \lesssim n_e$) the κ function presents a peculiar shape coming from the interplay between the self-induced and the matter effects with a comparable strength. The κ curve broadens at smaller r with respect to the case with $n_e = 0$. The peak of κ is slightly reduced by the matter effects. However, its position remains the same, giving the onset of the flavor conversions found numerically. At later times, when n_e dominates over $n_{\bar\nu_e}$, the matter suppression becomes more relevant. However, since at most $n_e \gtrsim 2n_{\bar\nu_e}$, the suppression is never as strong as in the case of the iron-core SNe. Also in this case, the matter effect shifts at larger radii the onset of the flavor conversions.

V. CONCLUSIONS

We have performed a linear stability analysis of the self-induced flavor conversions during the accretion phase for two SN models with different progenitor masses. We characterize the SN densities, the neutrino energy and angular spectra, with results from recent SN hydrodynamical simulations. We compared this method with the numerical results of the flavor evolution presented in our previous paper [27], where we assumed a schematic ν emission, with that all the neutrinos streaming half-isotropically from the neutrino-sphere with a single representative energy. For the case of an iron-core 10.8 $M_\odot$ SN (and 18.0 $M_\odot$, not shown) we found that the continuous ν energy spectra do not play a crucial role in the issue of the stability of the neutrino ensemble with respect to our previous single-energy results. Conversely, the presence of forward-peaked ν angular distributions significantly reduces the strength of the ν-ν interaction term. This effect would enhance the suppression of the self-induced oscillations, due to the dense matter term. We find that the flavor instability is completely suppressed for large part of the duration of the accretion phase, excepct for a small time window around $t_{\rm pb} \sim 0.3$ s. However, we checked with multi-energy and multi-angle simulations that the effect of these partial flavor conversions would be negligible in the characterization of the observable supernova neutrino flux. Our result is in agreement with the stability analysis recently performed with a 15.0 $M_\odot$ SN model from the Garching group [30]. In that paper, a complete matter suppression of the self-induced flavor conversions was found for all the duration of the accretion phase. In the case of a low-mass O-Ne-Mg SN with 8.8 $M_\odot$ progenitor, where the accretion phase is extremely short, the matter density profile is lower and the ν angular distributions less forward-peaked than in iron-core models. As a consequence, we found that also with realistic angular distributions flavor conversions would be possible at early times, i.e. at $t_{\rm pb} \lesssim 0.2$ s. The different pattern of the self-induced flavor conversions for these two SN progenitors could be, at least in principle, a tool to distinguish between iron-core and O-Ne-Mg core SNe.

The matter suppression of the self-induced flavor conversions for iron-core supernovae would imply that the original neutrino spectra will be processed only by the ordinary Mikheyev-Smirnov-Wolfenstein effect in the outer stellar layers. This effect would allow to distinguish the neutrino mass hierarchy through the Earth matter effects [47] or the rise time of the SN neutrino signal [48], in the case of a θ_{13} neutrino mixing angle as "large" as currently measured by the Daya Bay [49] and Reno [50] reactor experiments. These recent measurement confirm and greatly strengthen the significance of early hints suggested by the long-baseline ν_μ-ν_e experiments [51, 52] and Double Chooz reactor experiment [53], especially when analysed in combination with other oscillation data [54]. This intriguing consequence implies that the characterization of the ν flavor evolution during the accretion phase

is crucial for the interpretation of the observable SN ν signal. At this regard in [29], due to a different choice of the neutrino angular distributions, a less pronounced matter suppression has been found for iron-core SNe. In future it will be mandatory to apply the stability analysis also to other SN models in order to understand how generic are the results obtained till now.

Acknowledgements

We thank P.D. Serpico for interesting discussions during the development of this project. We also acknowledge G. Raffelt and G. Sigl for reading the manuscript and for useful comments on it. The work of S.C., A.M., N.S. was supported by the German Science Foundation (DFG) within the Collaborative Research Center 676 "Particles, Strings and the Early Universe". T.F. acknowledges support from the Swiss National Science Foundation (SNF) under grant no. PBBSP2-133378 and HIC for FAIR.

References

[1] G. Raffelt, "Neutrinos and the stars," arXiv:1201.1637 [astro-ph.SR].
[2] B. Dasgupta, "Physics and Astrophysics Opportunities with Supernova Neutrinos," PoS ICHEP **2010**, 294 (2010) [arXiv:1005.2681 [hep-ph]].
[3] G. M. Fuller and Y. Z. Qian, "Simultaneous Flavor Transformation of Neutrinos and Antineutrinos with Dominant Potentials from Neutrino-Neutrino Forward Scattering," Phys. Rev. D **73**, 023004 (2006) [astro-ph/0505240].
[4] H. Duan, G. M. Fuller and Y. Z. Qian, "Collective Neutrino Flavor Transformation In Supernovae," Phys. Rev. D **74**, 123004 (2006) [astro-ph/0511275].
[5] H. Duan, G. M. Fuller, J. Carlson and Y. Z. Qian, "Simulation of coherent non-linear neutrino flavor transformation in the supernova environment. I: Correlated neutrino trajectories," Phys. Rev. D **74**, 105014 (2006) [astro-ph/0606616].
[6] G. L. Fogli, E. Lisi, A. Marrone and A. Mirizzi, "Collective neutrino flavor transitions in supernovae and the role of trajectory averaging," JCAP **0712**, 010 (2007) [arXiv:0707.1998 [hep-ph]].
[7] B. Dasgupta and A. Dighe, "Collective three-flavor oscillations of supernova neutrinos," Phys. Rev. D **77**, 113002 (2008) [arXiv:0712.3798 [hep-ph]].
[8] B. Dasgupta, A. Dighe, G. G. Raffelt and A. Y. Smirnov, "Multiple Spectral Splits of Supernova Neutrinos," Phys. Rev. Lett. **103**, 051105 (2009) [arXiv:0904.3542 [hep-ph]].
[9] R. F. Sawyer, "The multi-angle instability in dense neutrino systems," Phys. Rev. D **79**, 105003 (2009) [arXiv:0803.4319 [astro-ph]].
[10] A. Friedland, "Self-refraction of supernova neutrinos: mixed spectra and three-flavor instabilities," Phys. Rev. Lett. **104**, 191102 (2010) [arXiv:1001.0996 [hep-ph]].
[11] B. Dasgupta, G. G. Raffelt and I. Tamborra, "Triggering collective oscillations by three-flavor effects," Phys. Rev. D **81**, 073004 (2010) [arXiv:1001.5396 [hep-ph]].
[12] B. Dasgupta, A. Mirizzi, I. Tamborra and R. Tomàs, "Neutrino mass hierarchy and three-flavor spectral splits of supernova neutrinos," Phys. Rev. D **81**, 093008 (2010) [arXiv:1002.2943 [hep-ph]].
[13] H. Duan and A. Friedland, "Self-induced suppression of collective neutrino oscillations in a supernova," Phys. Rev. Lett. **106**, 091101 (2011) [arXiv:1006.2359 [hep-ph]].
[14] A. Mirizzi and R Tomàs, "Multi-angle effects in self-induced oscillations for different supernova neutrino fluxes," Phys. Rev. D **84**, 033013 (2011) [arXiv:1012.1339 [hep-ph]].
[15] Y. Pehlivan, A. B. Balantekin, T. Kajino and T. Yoshida, "Invariants of Collective Neutrino Oscillations," Phys. Rev. D **84**, 065008 (2011) [arXiv:1105.1182 [astro-ph.CO]].
[16] J. T. Pantaleone, "Neutrino Flavor Evolution Near A Supernova's Core," Phys. Lett. B **342**, 250 (1995) [astro-ph/9405008].
[17] Y. Z. Qian, G. M. Fuller, G. J. Mathews, R. Mayle, J. R. Wilson and S. E. Woosley, "A Connection Between Flavor Mixing Of Cosmologically Significant Neutrinos And Heavy Element Nucleosynthesis In Supernovae," Phys. Rev. Lett. **71**, 1965 (1993).
[18] Y. Z. Qian and G. M. Fuller, "Neutrino-neutrino scattering and matter enhanced neutrino flavor transformation in Supernovae," Phys. Rev. D **51**, 1479 (1995) [astro-ph/9406073].
[19] S. Pastor and G. Raffelt, "Flavor oscillations in the supernova hot bubble region: Nonlinear effects of neutrino background," Phys. Rev. Lett. **89**, 191101 (2002) [astro-ph/0207281].
[20] S. Hannestad, G. G. Raffelt, G. Sigl and Y. Y. Y. Wong, "Self-induced conversion in dense neutrino gases: Pendulum in flavour space," Phys. Rev. D **74**, 105010 (2006) [Erratum-ibid. D **76**, 029901 (2007)] [astro-ph/0608695].
[21] G. G. Raffelt and A. Y. Smirnov, "Self-induced spectral splits in supernova neutrino fluxes," Phys. Rev. D **76**, 081301 (2007) [Erratum-ibid. D **77**, 029903 (2008)] [arXiv:0705.1830 [hep-ph]].
[22] G. G. Raffelt, A. Y. Smirnov, "Adiabaticity and spectral splits in collective neutrino transformations," Phys. Rev. **D76**, 125008 (2007). [arXiv:0709.4641 [hep-ph]].
[23] H. Duan, G. M. Fuller, J. Carlson and Y. Q. Zhong, "Neutrino Mass Hierarchy and Stepwise Spectral Swapping of Supernova Neutrino Flavors," Phys. Rev. Lett. **99**, 241802 (2007). [arXiv:0707.0290 [astro-ph]].
[24] H. Duan, G. M. Fuller and Y. Z. Qian, "Collective Neutrino Oscillations," Ann. Rev. Nucl. Part. Sci. **60**, 569 (2010) [arXiv:1001.2799 [hep-ph]].
[25] A. Esteban-Pretel, A. Mirizzi, S. Pastor, R. Tomàs, G. G. Raffelt, P. D. Serpico and G. Sigl, "Role of dense

matter in collective supernova neutrino transformations," Phys. Rev. D **78**, 085012 (2008) [arXiv:0807.0659 [astro-ph]].

[26] S. Chakraborty, T. Fischer, A. Mirizzi, N. Saviano and R. Tomàs, "No collective neutrino flavor conversions during the supernova accretion phase," Phys. Rev. Lett. **107**, 151101 (2011) [arXiv:1104.4031 [hep-ph]].

[27] S. Chakraborty, T. Fischer, A. Mirizzi, N. Saviano and R. Tomàs, "Analysis of matter suppression in collective neutrino oscillations during the supernova accretion phase," Phys. Rev. D **84**, 025002 (2011) [arXiv:1105.1130 [hep-ph]].

[28] T. Fischer, S. C. Whitehouse, A. Mezzacappa, F. K. Thielemann and M. Liebendörfer, "Protoneutron star evolution and the neutrino driven wind in general relativistic neutrino radiation hydrodynamics simulations," Astron. Astrophys. **517**, A80 (2010). [arXiv:0908.1871 [astro-ph.HE]].

[29] B. Dasgupta, E. P. O'Connor and C. D. Ott, "The Role of Collective Neutrino Flavor Oscillations in Core-Collapse Supernova Shock Revival," Phys. Rev. D **85**, 065008 (2012) [arXiv:1106.1167 [astro-ph.SR]].

[30] S. Sarikas, G. G. Raffelt, L. Hudepohl and H. T. Janka, "Suppression of Self-Induced Flavor Conversion in the Supernova Accretion Phase," Phys. Rev. Lett. **108**, 061101 (2012) [arXiv:1109.3601 [astro-ph.SR]].

[31] S. Sarikas and G. Raffelt, "Flavor stability analysis of supernova neutrino fluxes compared with simulations," arXiv:1110.5572 [astro-ph.SR].

[32] A. Banerjee, A. Dighe and G. Raffelt, "Linearized flavor-stability analysis of dense neutrino streams," Phys. Rev. D **84**, 053013 (2011) [arXiv:1107.2308 [hep-ph]].

[33] K. Nomoto, "Evolution of 8–10 $M_\odot$ stars toward electron capture supernovae. I. Formation of electron-degenerate O + Ne + Mg cores," Astrophys. J. **277**, 791 (1984).

[34] K. Nomoto, "Evolution of 8–10 $M_\odot$ stars toward electron capture supernovae. II. Collapse of an O + Ne + Mg core," Astrophys. J. **322**, 206 (1987).

[35] F. S. Kitaura, H.-Th. Janka and W. Hillebrandt, "Explosions of O-Ne-Mg cores, the crab supernova, and subluminous type II-p supernovae " Astron. Astrophys. **450**, 345 (2006).

[36] S. E. Woosley, A. Heger and T. A. Weaver, "The evolution and explosion of massive stars," Rev. Mod. Phys. **74**, 1015 (2002).

[37] C. D. Ott, A. Burrows, L. Dessart and E. Livne, "2D Multi-Angle, Multi-Group Neutrino Radiation-Hydrodynamic Simulations of Postbounce Supernova Cores," Astrophys. J. **685**, 1069 (2008) [arXiv:0804.0239 [astro-ph]].

[38] A. Esteban-Pretel, S. Pastor, R. Tomàs, G. G. Raffelt and G. Sigl, "Decoherence in supernova neutrino transformations suppressed by deleptonization," Phys. Rev. D **76**, 125018 (2007) [arXiv:0706.2498 [astro-ph]].

[39] M. T. Keil, G. Raffelt, H.-T. Janka, "Monte Carlo study of supernova neutrino spectra formation," Astrophys. J. **590**, 971 (2003) [astro-ph/0208035].

[40] G. G. Raffelt, M. T. Keil, R. Buras, H. T. Janka and M. Rampp, "Supernova neutrinos: Flavor-dependent fluxes and spectra," arXiv:astro-ph/0303226.

[41] T. Fischer, G. Martinez-Pinedo, M. Hempel and M. Liebendorfer, "Neutrino spectra evolution during proto-neutron star deleptonization," Phys. Rev. D **85**, 083003 (2012) [arXiv:1112.3842 [astro-ph.HE]].

[42] A. Mirizzi and P. D. Serpico, "Instability in the dense supernova neutrino gas with flavor-dependent angular distributions," arXiv:1110.0022 [hep-ph].

[43] T. -K. Kuo and J. T. Pantaleone, "Neutrino Oscillations in Matter," Rev. Mod. Phys. **61**, 937 (1989).

[44] G. Sigl and G. Raffelt, "General kinetic description of relativistic mixed neutrinos," Nucl. Phys. B **406**, 423 (1993).

[45] J. T. Pantaleone, "Neutrino oscillations at high densities," Phys. Lett. B **287**, 128 (1992).

[46] L. Wolfenstein, "Neutrino Oscillations In Matter," Phys. Rev. D **17**, 2369 (1978); S. P. Mikheev and A. Yu. Smirnov, "Resonance Enhancement Of Oscillations In Matter And Solar Neutrino Spectroscopy," Yad. Fiz. **42**, 1441 (1985) [Sov. J. Nucl. Phys. **42**, 913 (1985)].

[47] A. S. Dighe, M. T. Keil and G. G. Raffelt, "Identifying earth matter effects on supernova neutrinos at a single detector," JCAP **0306**, 006 (2003) [hep-ph/0304150].

[48] P. D. Serpico, S. Chakraborty, T. Fischer, L. Hudepohl, H. -T. Janka, and A. Mirizzi, "Probing the neutrino mass hierarchy with the rise time of a supernova burst," Phys. Rev. D **85**, 085031 (2012) [arXiv:1111.4483 [astro-ph.SR]].

[49] F. P. An *et al.* [DAYA-BAY Collaboration], "Observation of electron-antineutrino disappearance at Daya Bay," Phys. Rev. Lett. **108**, 171803 (2012) [arXiv:1203.1669 [hep-ex]].

[50] J. K. Ahn *et al.* [RENO Collaboration], "Observation of Reactor Electron Antineutrino Disappearance in the RENO Experiment," arXiv:1204.0626 [hep-ex].

[51] K. Abe *et al.* [T2K Collaboration], "Indication of Electron Neutrino Appearance from an Accelerator-produced Off-axis Muon Neutrino Beam," Phys. Rev. Lett. **107**, 041801 (2011) [arXiv:1106.2822 [hep-ex]].

[52] P. Adamson *et al.* [MINOS Collaboration], "Improved search for muon-neutrino to electron-neutrino oscillations in MINOS," Phys. Rev. Lett. **107**, 181802 (2011) [arXiv:1108.0015 [hep-ex]].

[53] Y. Abe *et al.* [DOUBLE-CHOOZ Collaboration], "Indication for the disappearance of reactor electron antineutrinos in the Double Chooz experiment," Phys. Rev. Lett. **108**, 131801 (2012) [arXiv:1112.6353 [hep-ex]].

[54] G. L. Fogli, E. Lisi, A. Marrone, A. Palazzo and A. M. Rotunno, "Evidence of theta(13)>0 from global neutrino data analysis," Phys. Rev. D **84**, 053007 (2011) [arXiv:1106.6028 [hep-ph]].